

### Formation Mechanism Dependence on Laser Power of UV-laser Ablated Silicon Surface Gratings

**Cheng-Yen Chen, Steffen Gurtler, C. C. Yang**

Institute of Electro-Optical Engineering, National Taiwan University,  
1, Roosevelt Road, Sec. 4, Taipei, Taiwan, R.O.C.

(Tel) 886-2-23657624 (Fax) 886-2-23652637 (E-mail) ccy@cc.ee.ntu.edu.tw

**Kung-Jeng Ma**

Department of Mechanical Engineering, Chung Cheng Institute of Technology,  
Ta-Shi, Taoyuan, Taiwan, R.O.C.

Silicon surface gratings are useful for temperature control in IC process and optoelectronics applications. They can be easily fabricated with laser ablation. In this paper, we report our results of UV-laser ablated silicon surface gratings. It was found that different laser-matter interactions were involved for forming the surface gratings when different levels of laser power were used. Hence, different morphologies of gratings were observed. In fabricating a grating, a silicon wafer was exposed to the interference fringes formed through a prism or a holographic system with the fourth-harmonic (266 nm) of a Q-switched Nd:YAG laser. With the prism method, the grating period can be varied from 180 through 600 nm. Figure 1 shows the atomic force microscopic (AFM) picture of a silicon surface grating with the period at 400 nm. The grating was formed with 14 mJ/cm<sup>2</sup> laser fluence with 30 Hz pulse repetition rate for 15 sec (i.e., 450 pulse shots) in the atmosphere. It was identified that the formation of the corrugations was due to silicon oxidation process. The crests shown in the figure are silicon oxide. From the Fourier transform infrared spectroscopy study, the oxide is oxygen deficient, i.e., SiO<sub>x</sub> (x < 2). Also, it was discovered that the oxidation process would be more efficient with ambient water vapor, compared with ambient oxygen molecules. The existence of oxide was proved with energy dispersive X-ray spectroscopy and HF etching. Figure 2 shows the AFM picture of the grating of Fig. 1 after HF dipping. After silicon oxide was removed, the crests became valleys. Figure 3 shows the real-time monitoring of the first-order diffracted signal intensity variation with number of laser shots. The results were obtained using the holographic system. We can see that the diffraction becomes detectable after 700 shots in this situation. The slightly irregular variation of the diffracted intensity was attributed to mechanical instability. To see the dependence on laser power level, we increased the laser fluence to 60 mJ/cm<sup>2</sup>. Figure 4 shows the diffracted intensity variation with the number of laser shots. The spiky features shown here are similar with ambient water vapor and ambient nitrogen, indicating that the rapid formation and destruction have nothing to do with silicon oxidation. It is believed that this process is due to quick melting and sputtering. Again, the destruction of grating is caused by mechanical instability. To further understand this ablation process, we exposed the sample with only one laser shot at 60 mJ/cm<sup>2</sup>. Because of aberration in our laser interference system, a fringe of a larger period was formed besides the designated interference fringe. Figures 5 and 6 show the AFM pictures of the grating at a high and a low intensity beam portions, respectively. From Fig. 5, we can see that at the highest intensity sharp peaks with valleys on both sides were formed. Then, at the medium intensity double peaks with three valleys were produced. At the lowest intensity, nothing is visible. Note that after HF dipping, the structures in Figs. 5 and 6 still existed, indicating that their formation was not due to silicon oxidation. More detailed results, including the data of energy dispersive X-ray spectroscopy and the origins of the different surface morphologies, will be discussed.

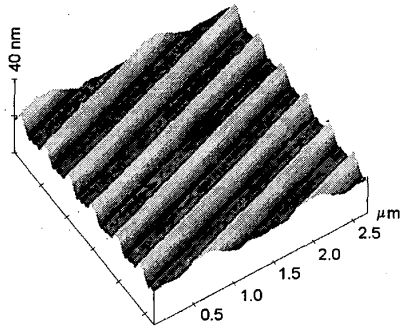


Fig. 1 AFM picture of an oxide grating.

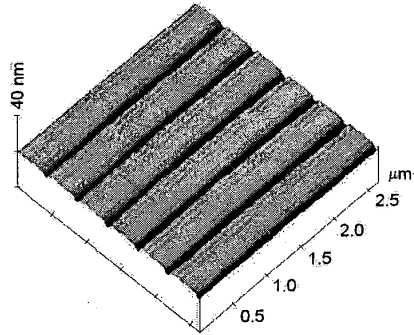


Fig. 2 AFM picture after HF dipping.

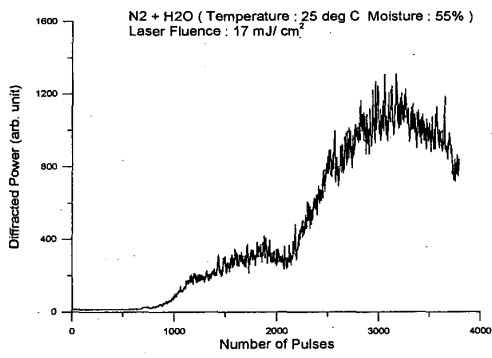


Fig. 3 Growth of an oxide grating.

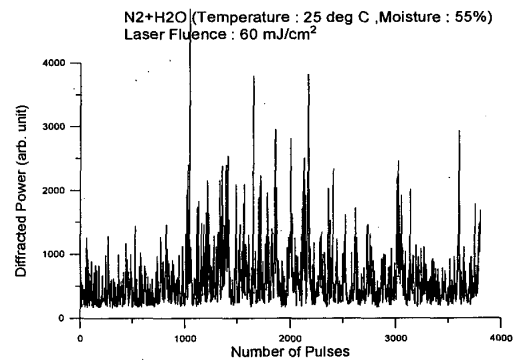


Fig. 4 Evolution of an ablated grating.

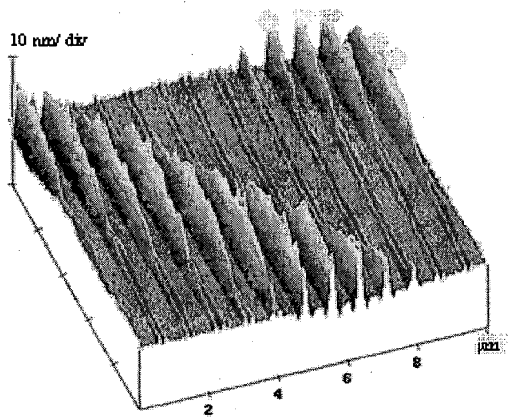


Fig.5 AFM picture after single-shot exposure.

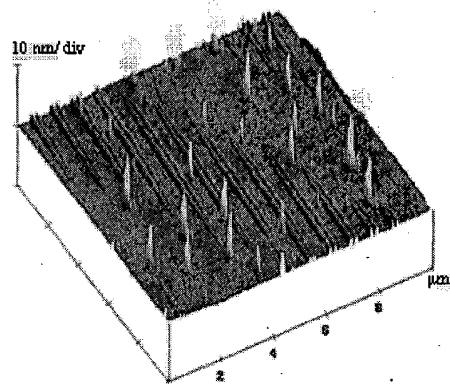


Fig. 6 AFM picture of another portion.